Elucidating the Influence of Anchoring Geometry on the Reactivity of NO_2-Functionalized N-Heterocyclic Carbene Monolayers

Shahar Dery[a], Suhong Kim[b], Gabriele Tomaschun[c], Iris Berg[a], Daniel Feferman[a], Albano Cossaro[d], Alberto Verdini[d], Luca Floreano[d], Thorsten Klüner[c], F. Dean Toste[b] and Elad Gross*[a]*

[a] Institute of Chemistry and The Center for Nanoscience and Nanotechnology, The Hebrew University of Jerusalem, Jerusalem 91904, Israel

[b] Department of Chemistry, University of California, Berkeley, California 94720, United States

[c] Department of Chemistry, Carl von Ossietzky University Oldenburg, 26111 Oldenburg, Germany

[d] CNR-IOM, Laboratorio Nazionale TASC, Basovizza SS-14, Trieste 34012, Italy

Corresponding Author

* F. Dean Toste: fdtoste@berkeley.edu

* Elad Gross: elad.gross@mail.huji.ac.il

ABSTRACT

The development of chemically-addressable N-heterocyclic carbene (NHC) based self-assembled monolayers (SAMs) requires in-depth understanding of the influence of NHCs anchoring geometry on its chemical functionality. Herein, it is demonstrated that the chemical reactivity of surface anchored NO_2-functionalized NHCs (NO_2-NHCs) can be tuned by modifying the distance between the functional group and the reactive surface, which is governed by the deposition technique. Liquid-deposition of NO_2-NHCs on Pt (111) induced a SAM in which the NO_2-aryl groups were flat-lying on the surface. The high proximity between the NO_2 groups and the Pt surface led to high reactivity and 85% of the NO_2 groups were reduced at room temperature. Lower reactivity was obtained with vapor-deposited NO_2-NHCs that assumed a preferred upright geometry. The separation between the NO_2 groups in the vapor-deposited NO_2-NHCs and the reactive surface circumvented their surface-induced reduction, which was facilitated only after exposure to harsher reducing conditions.

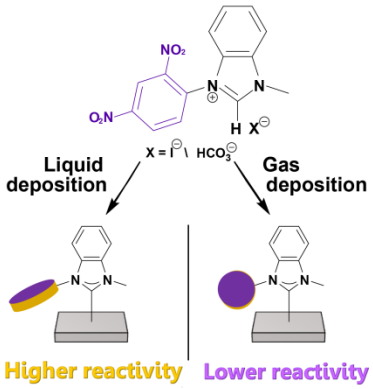

KEYWORDS Self-assembled monolayers; N-Heterocyclic Carbene; NEXAFS; Anchoring geometry;

The high chemical tunability and metal-affinity of N-heterocyclic carbene molecules (NHCs) have enabled to form robust NHCs-based self-assembled monolayers (SAMs) with exceptional stability and functionality.[1-10] Chemically-functionalized NHCs have been utilized for the formation of SAMs with varied applications range, including molecular patterning, biosensing and catalysis.[11-16]

Two main approaches have been developed for surface-anchoring of NHCs: 1. Liquid-deposition; in which deprotonation is facilitated by a strong base, such as potassium tert-butoxide (KO^tBu), for the formation of an active carbene that can be anchored on metallic surfaces (Scheme 1a).[12, 17] 2. Vapor-deposition; in this approach hydrogen carbonates counteranion serves as a base for deprotonation of the imidazolium cation, enabling active carbene formation and its surface-anchoring under ultra-high vacuum (UHV) conditions (Scheme 1b).[11]

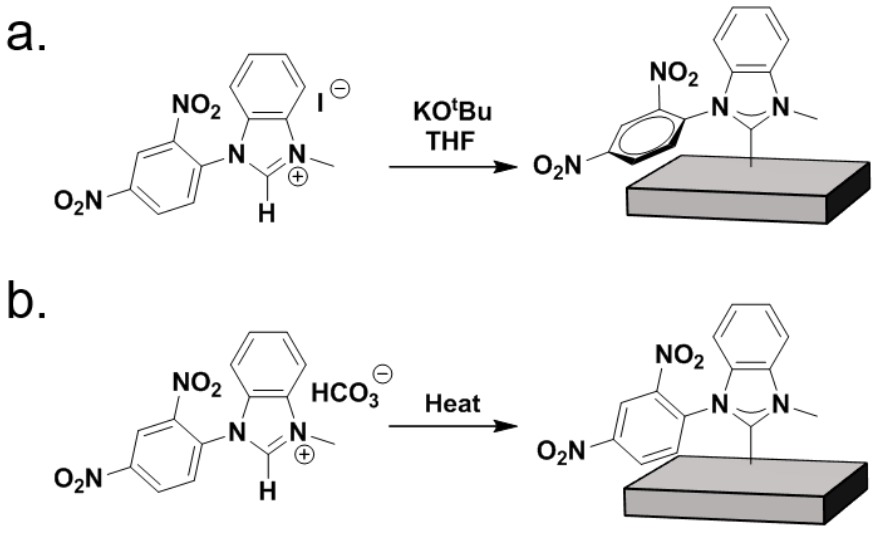

Scheme 1. Schematic illustration of liquid- (**a**) and vapor-deposition (**b**) of NO_2-functionalized NHCs.

It was demonstrated that a more homogeneous and better stabilized SAM is formed by vapor-deposition, in comparison to the one prepared by liquid-deposition.[11, 18] However, the influence of the deposition technique on the anchoring geometry of surface-anchored NHCs, which is expected to have a crucial impact on the functionality of chemically-addressable NHCs, was not yet elucidated. In this work we demonstrate that the anchoring geometry has a direct influence on the chemical reactivity of NO_2-functionalized NHCs (NO_2-NHCs) and that by changing the deposition technique both the anchoring geometry and chemical reactivity of NHCs-based SAM can be tuned.

Liquid deposition of NO_2-NHCs on Pt (111) was performed by using potassium tert-butoxide (KO^tBu) as a base for deprotonation of the tetrahydrofuran (THF) dissolved imidazolium salt (scheme 1a). The anchoring geometry, chemical reactivity and thermal stability of the SAM were identified by conducting X-ray photoelectron spectroscopy (XPS) and near-edge X-ray absorption fine structures (NEXAFS) measurements (performed at ALOISA beamline of the ELETTRA synchrotron facility in Trieste, Italy)[19-20], along with complementary density functional theory (DFT) calculations. Additional details about the NHCs synthesis, the experimental setup and DFT calculations are described in the supporting information.

N1s XPS signal of liquid-deposited NO_2-NHCs on Pt (111) is shown in Fig. 1a. The wide (FWHM = 3 eV) low energy peak (397-404 eV) revealed the presence of various nitrogen species on the surface. The peak was fit by four Gaussians centered at 398.5, 399.8, 401.1 and 402.3 eV, which were assigned to pyridinic (C–N=C), amine ($C–NH_2$/C=NH), pyrrolic (N=C) and protonated amine ($–NH_3^+$), respectively.[21-24]

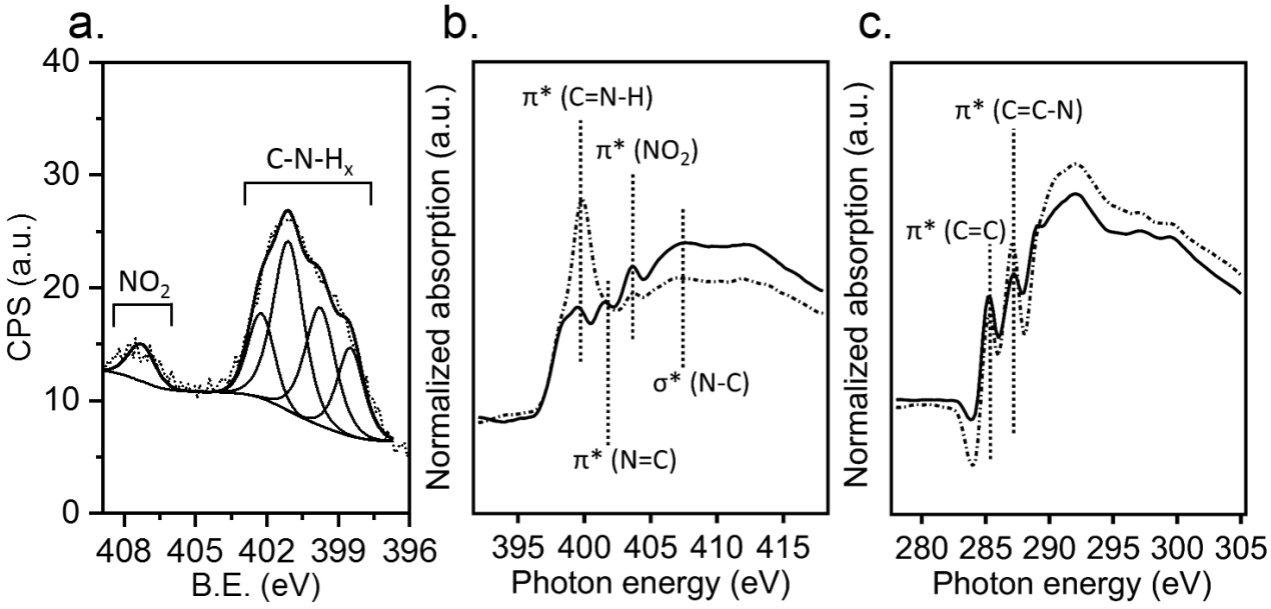

Figure 1. Spectroscopic characterization of liquid-deposited NO_2-NHC on Pt (111). **a.** N1s XPS spectrum **b.** Nitrogen k-edge NEXAFS spectra. **c.** Carbon k-edge NEXAFS spectra. NEXAFS spectra were acquired at both p- and s-polarization (marked by solid and dotted lines, respectively).

The high energy N1s XPS peak (406-409 eV) was fit by one Gaussian and correlated to NO_2 species. The low to high energy N1s XPS peaks area ratio was 1:10 while the expected ratio, based on the molecular structure of NO_2-NHC, is 1:1, indicating that 85% of the NO_2 groups were reduced (Table 1). The XPS results revealed that partial decomposition and nitro-groups reduction have occurred following liquid-deposition of NO_2-NHCs on the Pt surface. These two processes were facilitated by residue H_2 molecules, which were the main gas component in the UHV chamber.

Nitrogen and carbon k-edge NEXAFS measurements (Fig. 1b and 1c, respectively) were conducted at both p- and s-polarization (marked by solid and dotted lines, respectively) to determine the anchoring geometry of liquid-deposited NO_2-NHCs. The p-polarized nitrogen k-

edge NEXAFS spectrum (solid line, Fig. 1b) displayed three dominant peaks in the π* region (395-405 eV). The peak at 403.6 eV was correlated to N1s → $\pi^*_{(NO2)}$ transitions, while the peak at 401.5 eV was assigned to N1s → $\pi^*_{(N=C)}$ transition and the peak at 399.7 eV was correlated to N1s → $\pi^*_{(C=N-H)}$ transition.[25-26] Interestingly, the s-polarized spectrum (dotted line) revealed a much more intense N1s → $\pi^*_{(C=N–H)}$ transition while the N1s → $\pi^*_{(NO2)}$ transition peak was higher in the p-polarized spectrum. These differences indicate that the $–NO_2$ groups obtained a preferred parallel orientation to the surface, while the reduced groups were mostly oriented perpendicularly to the surface. The p- and s-polarized carbon k-edge NEXAFS spectra of liquid-deposited NO_2-NHCs (solid and dotted lines in Fig. 1c, respectively) included two π* transitions at 285.3 and 286.5 eV corresponding to C1s → $\pi^*_{(C=C)}$ and $\pi^*_{(C=C–N)}$ transitions, respectively.[26-27] The two π* transition peaks were almost identical in their position and amplitudes in both the p- and s-polarized spectra.

Table 1. XPS peaks area analysis

		N_{1s}/ Pt_{4f}	C_{1s}/ Pt_{4f}	C_{1s}/N_{1s}	NO_2: NH_x
Liquid deposition	As-deposited	0.06	0.35	5.48	15:85
Vapor deposition	As-deposited	0.04	0.11	3.05	40:60
	After reduction	0.04	0.10	2.97	5:95

DFT calculations were conducted to identify the preferred anchoring geometry and adsorption energy of liquid-deposited NHCs on Pt (111) surface and Pt (111) surface decorated with a Pt ad-atom (Pt-ad/Pt(111)) (Fig. 2a and Supp. Info. Fig. S1). The optimal anchoring site for NO_2-

NHCs was on Pt ad-atom (E_{ads}= -4.94 eV) in which the NO_2-aryl orientation was mostly flat-lying on the surface, while the imidazole ring was oriented in a standing position (see further adsorption analysis in Supp. Info. Fig. S1). The DFT results nicely corroborate the experimental data, revealing that the similarities between the p- and s-polarized carbon NEXAFS spectra are due to the fact that the two phenyl rings are positioned at 90° to each other. It should be noted that DFT calculations identified that reduction of the $–NO_2$ groups do not noticeably influence the NHCs anchoring geometry (Fig. 2b and Supp. Info Fig S1). The identification of Pt ad-atom as the most favorable adsorption site for NO_2-NHCs on Pt (111) surface indicates that NO_2-NHCs adsorption will lead to restructuring of the Pt surface.[3,7,28]

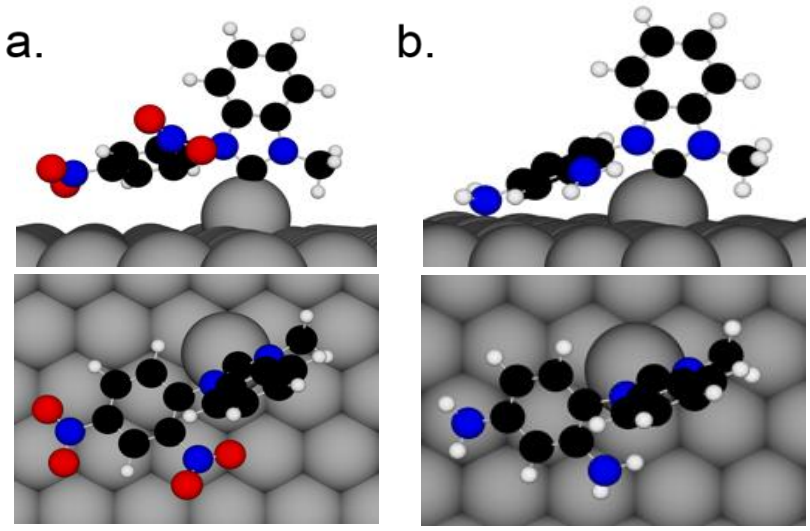

Figure 2. DFT calculations of the optimized adsorption geometry of NO_2-NHC (**a**) and NH_2-NHC (**b**) on Pt-ad/Pt (111) (Pt (111) surface decorated with a Pt ad-atom). Side and top views of the NHCs are shown (top and bottom panels, respectively).

Vapor-deposition of NO_2-NHCs on Pt (111) surface was conducted under UHV conditions by thermal evaporation of NO_2-fucntionalized carbonate-imidazolium salt (Scheme 1b).[29] N1s XPS

spectrum of vapor-deposited NO_2-NHCs on Pt (111) is shown in Fig. 3a (black colored spectrum). The low energy N1s XPS peak was constructed of two dominant Gaussians, as expected from the molecular structure of the NO_2-NHC. The low to high energy N1s XPS peaks area ratio in vapor-deposited NO_2-NHCs was 1:5, indicating that 60% of the NO_2 groups were reduced upon NHCs deposition (Table 1). These results reveal that NO_2-NHCs that were anchored on the surface by vapor-deposition show lower affinity toward $–NO_2$ reduction and partial decomposition, in comparison to NO_2-NHCs that were liquid-deposited on the Pt surface. Based on these results it can be deduced that vapor-deposition is a less destructive technique, in comparison to liquid-deposition, for surface-anchoring of NO_2-NHCs.

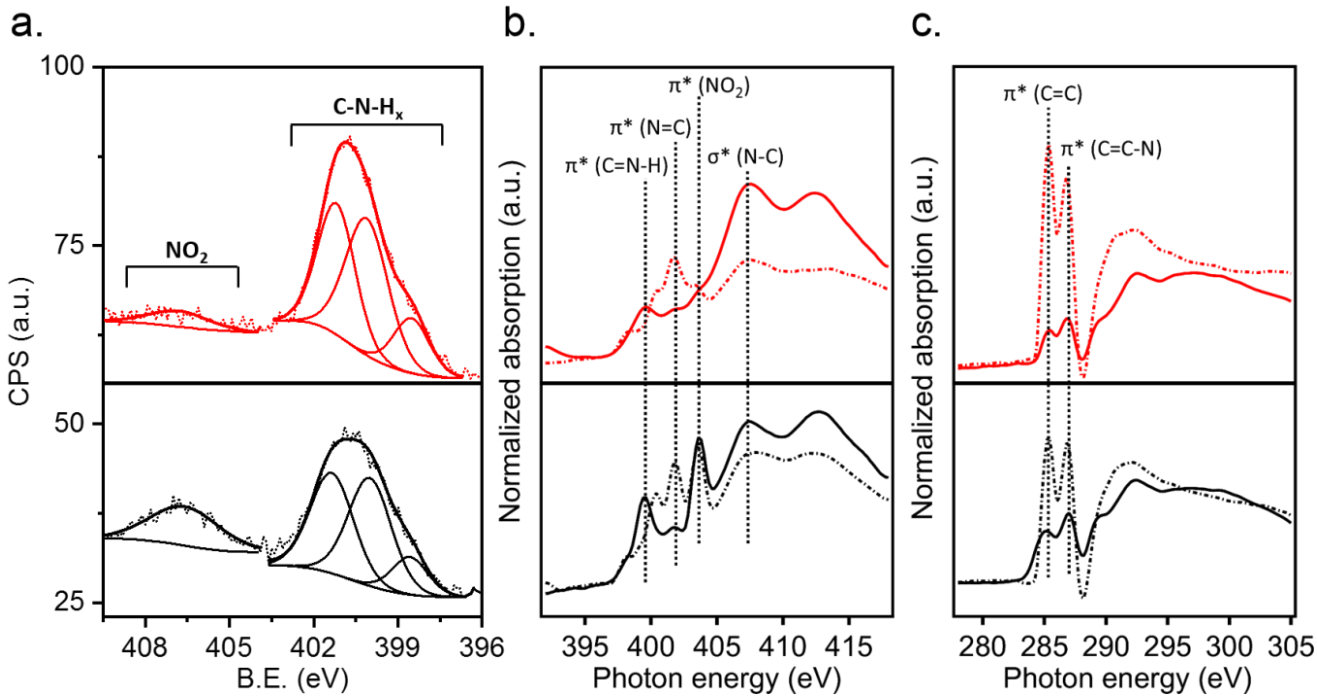

Figure 3. Spectroscopic characterization of vapor-deposited NO_2-NHCs on Pt (111) before (black-colored spectrum) and after (red-colored spectrum) exposure to 1000 L of H_2 at 100 °C. **a.** N1s XPS spectrum **b.** Nitrogen k-edge NEXAFS spectra. **c.** Carbon k-edge NEXAFS spectra. NEXAFS spectra were acquired at both p- and s-polarization (marked by solid and dotted lines, respectively).

The anchoring-geometry of vapor-deposited NHCs was analyzed by conducting nitrogen and carbon k-edge NEXAFS measurements (Fig. 3b and 3c, respectively). P-polarized nitrogen k-edge NEXAFS spectrum (solid line, black colored spectrum in Fig. 3b) showed two intense peaks in the π* transition range, correlated to N 1s → $\pi^*_{(NO2)}$ (403.6 eV) and N 1s → $\pi^*_{(C=N-H)}$ (399.7 eV) transitions. While the position and amplitude of N 1s → $\pi^*_{(NO2)}$ transition was almost identical in both p- and s-polarized spectra (solid and dotted black colored spectra, respectively, Fig. 3b). The s-polarized spectrum showed an additional peak at 401.5 eV, correlated to N 1s → $\pi^*_{(N=C)}$ transition. This peak was not detected in the p-polarized spectrum. The σ* transition range (405-415 eV) was similar in its pattern and amplitude in both p- and s-polarized spectra.

Clear differences were obtained between the p- and s-polarized carbon k-edge NEXAFS spectra of vapor-deposited NHCs (solid and dotted black colored spectra, respectively, Fig. 3c). The dichroism implies that the C=C and C=C–N bonds constructing the benzimidazolium and NO_2-aryl rings have a preferred standing orientation. Thus, integration of the carbon and nitrogen NEXAFS results indicates that unlike liquid-deposited NHCs, the vapor-deposited NHCs showed a preferred perpendicular orientation to the surface.

DFT calculations revealed that perpendicular orientation is preferred once the surface density of NO_2-NHCs was increased (Fig. 4a and Supp. Info. Fig. S2). The stabilizing intermolecular π-π interactions between neighboring standing NO_2-NHCs compensated the weaker interaction between the Pt surface and the surface-anchored molecules in a standing position (E_{ads}= -4.35 eV). Due to steric hindrance, similar intermolecular π-π interactions cannot be formed between the imidazole rings of NHCs that were anchored on the surface with their nitroaryl group in a flat-lying position.

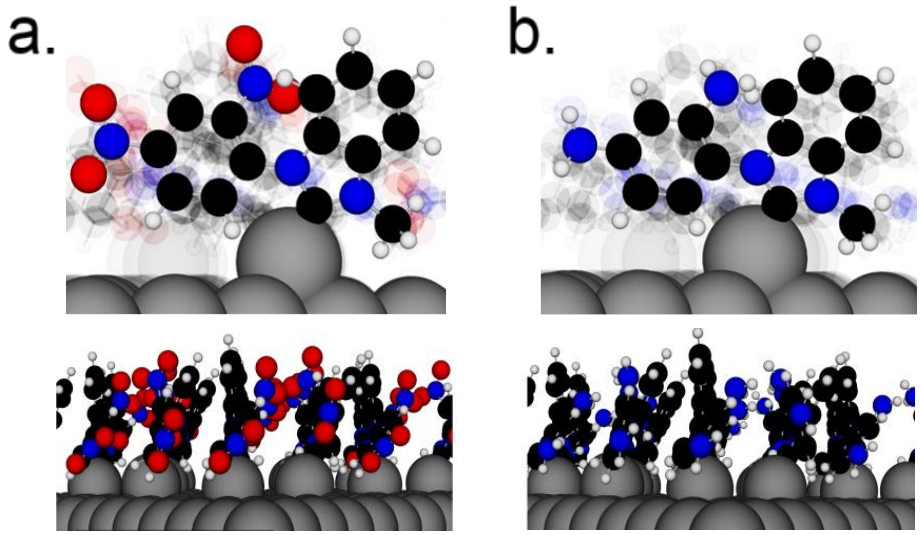

Figure 4. DFT calculations of the optimized adsorption geometry of NO_2-NHC (**a**) and NH_2-NHCs (**b**) on Pt-ad/Pt (111) with included intermolecular interactions. The lighter shading of other adsorbates on the surface illustrates the higher surface coverage, which is described in more detail in Supp. Info. Fig. S2. Front and side views of the surface-anchored NHCs are shown (top and bottom panels, respectively).

Integration of the experimental results and theoretical calculations specify that vapor-deposition enabled the formation of a highly-packed monolayer with strong intermolecular interactions in which the two NHC rings were oriented in a close to standing position. The high packing density of a monolayer constructed of NO_2-NHCs in a standing position makes it energetically favorable over a monolayer of flat-lying NO_2-NHCs, characterized with lower packing density due to steric hindrance.

The reasons for the formation of a monolayer of flat-lying NO_2-NHCs with lower packing density by the liquid-deposition approach can be correlated to either the presence of base residues on the surface or due to presence of encapsulated solvent molecules. The presence of potassium residues on the Pt surface was identified in the carbon k-edge NEXAFS measurements (Fig. 1c) in which two peaks at 296 and 298 eV were detected and correlated to potassium. The source for potassium was in KO^tBu that was used as a base in the liquid-deposition (Scheme 1a).

Distribution of potassium, and assumingly also $^{t}BuO^{-}$, on the Pt surface will limit the surface diffusivity of NHCs and thus hamper the formation of an ordered SAM with high packing density.[30-31]

Strong interactions between the activated NHCs and the THF molecules, required for dissolving the NHCs in the solution phase, can limit the surface diffusivity and modify the anchoring geometry of surface-anchored NHCs. Similarly, it was previously demonstrated that the packing density and anchoring geometry of thiol-based SAMs were influenced by the properties of the solvent used in the deposition process.[32-33] Indication for the presence of entrapped solvent molecules in the liquid-deposited monolayer was identified in quantitative analysis of the XPS spectra (Table 1). The C1s/N1s ratio in vapor-deposited NHCs was 3.05, which is comparable to the expected 3.5 carbon to nitrogen ratio in NO_2-NHC. However, the C1s/N1s ratio in the liquid-deposited NO_2-NHCs was 5.48, which is higher by 60% than the expected ratio. These results can be correlated to the presence of encapsulated solvent molecules in the liquid-deposited NHCs-based SAM. The encapsulation of solvent molecules in the SAM would hinder the formation of a monolayer with high packing density. The low packing density of NO_2-NHCs on the Pt surface will eventually induce a preferred flat-lying position of the nitroaryl substituents.

The variations in the anchoring geometry of vapor- and liquid-deposited NO_2-NHCs changed the distance between the $–NO_2$ groups and the reactive Pt surface. These differences impact the affinity toward surface induced reduction of the $–NO_2$ groups (Table 1). Higher probability towards nitro reduction was coupled with shorter distances and stronger interaction between the nitro groups and Pt surface. Thus, nitro reduction was facilitated in liquid-deposited NHCs, in which the two $–NO_2$ groups reside in high proximity to the Pt surface (Fig. 2a). Lower tendency

toward $–NO_2$ reduction was obtained in vapor-deposited NHCs, characterized with larger distances between the ortho $–NO_2$ group and the Pt surface (Fig. 4a).

To identify the influence of reducing conditions on the anchoring-geometry and nitro groups reducibility, the vapor-deposited NO_2-NHCs were exposed to 1000 L (L = Langmuir ; 1 L= 10^{-6} torr·sec) of H_2 at 100 °C. N1s XPS measurement revealed that the high energy peak was quenched following exposure of the vapor-deposited NHCs to reducing conditions (red colored spectrum, Fig. 3a). XPS peaks area ratio analysis showed that the $–NO_2$ reduction yield was increased from 60% to 95% following exposure to harsher reducing conditions (Table 1). The surface density of the NHCs did not noticeably change after exposure to reducing conditions, as obtained by the constant N1s/Pt4f ratio (Table 1), thus excluding any reduction-induced desorption of surface-anchored NHCs.

Nitrogen k-edge NEXAFS spectra (red colored spectra, Fig. 3b) showed that the N 1s $\rightarrow \pi^*_{(NO2)}$ (403.6 eV) and N 1s $\rightarrow \pi^*_{(C=N–H)}$ (399.7 eV) transitions were quenched after exposure to reducing conditions. These changes indicate that most of the nitro groups were fully reduced to amine following exposure to reducing conditions. Interestingly, a noticeable increase in the carbon k-edge dichroism was observed after exposure of the vapor-deposited NO_2-NHCs to reducing conditions (red colored spectra, Fig. 3c). The changes in the NEXAFS spectra revealed that the anchoring geometry of the NHCs was shifted to a more perpendicular position following NO_2 reduction. DFT calculations identified that nitro-groups reduction led to reorientation of the NHCs aromatic rings into a more upright position (Fig. 4b and Supp. Info Fig. S2). This is due to the fact that NO_2-reduction lowered the steric hindrance between the surface-anchored molecules, thus further enabling them to assume an optimized orientation.

In conclusion, the influence of anchoring geometry on the chemical reactivity of surface-anchored NO_2-NHCs was demonstrated by modifying the NHCs deposition technique. Liquid-deposition of NO_2-NHCs induced the formation of a SAM in which the nitro-aryl groups were flat-lying on the Pt surface. At this anchoring geometry the NO_2 reduction was facilitated under mild conditions due to the high proximity between the NO_2 groups and the Pt surface. Vapor-deposition led to the formation of NHCs-based SAM in which the NHCs assumed a favored standing orientation. The separation between the reactive surface and the NO_2 groups in the vapor-deposited NHCs circumvented their surface-induced reduction under mild conditions. The results presented herein demonstrate the impact of the distance between functional groups and the reactive surface on the reactivity of chemically-addressable SAMs. The anchoring geometry is therefore identified as a crucial factor that should be taken into consideration in the design of chemically-addressable SAMs.

ASSOCIATED CONTENT

Supporting Information includes additional DFT calculations and details about the experimental setup. The Supporting Information is available free of charge on the ACS Publications website.

ACKNOWLEDGMENT

This research was partially supported by the European Research Council (ERC) under the European Union's Horizon 2020 research and innovation program (Grant Agreement No. 802769, ERC Starting Grant “MapCat”) and by the State of Lower Saxony, Hannover, Germany. S.D. acknowledges financial support from the Israeli Ministry of Energy and the Azrieli foundation. F.D.T. thanks the Director, Office of Science, Office of Basic Energy Sciences and the Division of Chemical Sciences, Geosciences, and Biosciences of the US Department of

Energy at LBNL (DE-AC02-05CH11231) for partial support of this work. The theoretical calculations were performed at the HPC Clusters HERO and CARL, located at the University of Oldenburg and funded by the DFG through its Major Research Instrumentation Program (INST 184/108-1 FUGG and INST 184/157-1 FUGG) and the Ministry of Science and Culture of the Lower Saxony State. Computational analysis was also performed at the North-German Supercomputing Alliance (HLRN), within the project: nic00030.

REFERENCES

1. Zhukhovitskiy, A. V.; Mavros, M. G.; Van Voorhis, T.; Johnson, J. A. Addressable carbene anchors for gold surfaces. *J. Am. Chem. Soc.* **2013**, *135*, 7418-7421.

2. Crudden, C. M.; Horton, J. H.; Ebralidze, I. I.; Zenkina, O. V.; McLean, A. B.; Drevniok, B.; She, Z.; Kraatz, H.-B.; Mosey, N. J.; Seki, T. Ultra stable self-assembled monolayers of N-heterocyclic carbenes on gold. *Nat. Chem.* **2014**, *6*, 1755-4349.

3. Bakker, A.; Timmer, A.; Kolodzeiski, E.; Freitag, M.; Gao, H. Y.; Mönig, H.; Amirjalayer, S.; Glorius, F.; Fuchs, H. Elucidating the Binding Modes of N-Heterocyclic Carbenes on a Gold Surface. *J. Am. Chem. Soc.* **2018**, *140*, 11889-11892.

4. Li, Z.; Narouz, M. R.; Munro, K.; Hao, B.; Crudden, C. M.; Horton, J. H.; Hao, H. Carboxymethylated Dextran-Modified N-Heterocyclic Carbene Self-Assembled Monolayers on Gold for Use in Surface Plasmon Resonance Biosensing. *ACS Appl. Mater. Interfaces* **2017**, *9*, 39223-39234.

5. Lv, A.; Freitag, M.; Chepiga, K. M.; Schäfer, A. H.; Glorius, F.; Chi, L. N-Heterocyclic-Carbene-Treated Gold Surfaces in Pentacene Organic Field-Effect Transistors: Improved Stability and Contact at the Interface. *Angew. Chem., Int. Ed.* **2018**, *57*, 4792-4796.

6. Weidner, T.; Baio, J. E.; Mundstock, A.; Große, C.; Karthäuser, S.; Bruhn, C.; Siemeling, U. NHC-based self-assembled monolayers on solid gold substrates. *Aust. J. Chem* **2011**, *64*, 1177-1179.

7. Lovat, G.; Doud, E. A.; Lu, D.; Kladnik, G.; Inkpen, M. S.; Steigerwald, M. L.; Cvetko, D.; Hybertsen, M. S.; Morgante, A.; Roy, X. Determination of the structure and geometry of N-heterocyclic carbenes on Au (111) using high-resolution spectroscopy. *Chem. Sci.* **2019**, *10*, 930-935.

8. Larrea, C. R.; Baddeley, C. J.; Narouz, M. R.; Mosey, N. J.; Horton, J. H.; Crudden, C. M. N-Heterocyclic Carbene Self-assembled Monolayers on Copper and Gold: Dramatic Effect of Wingtip Groups on Binding, Orientation and Assembly. *ChemPhysChem* **2017**, *18*, 3536-3539.

9. Crespo, J.; Guari, Y.; Ibarra, A.; Larionova, J.; Lasanta, T.; Laurencin, D.; López-de-Luzuriaga, J. M.; Monge, M.; Olmos, M. E.; Richeter, S. Ultrasmall NHC-coated gold nanoparticles obtained through solvent free thermolysis of organometallic Au(i) complexes. *Dalton Trans.* **2014**, *43*, 15713-15718.

10. Rodríguez-Castillo, M.; Lugo-Preciado, G.; Laurencin, D.; Tielens, F.; van der Lee, A.; Clément, S.; Guari, Y.; López-de-Luzuriaga, J. M.; Monge, M.; Remacle, F. Experimental and Theoretical Study of the Reactivity of Gold Nanoparticles Towards Benzimidazole-2-ylidene Ligands. *Chem. - Eur. J.* **2016**, *22*, 10446-10458.

11. Crudden, C. M.; Horton, J. H.; Narouz, M. R.; Li, Z.; Smith, C. A.; Munro, K.; Baddeley, C. J.; Larrea, C. R.; Drevniok, B.; Thanabalasingam, B. Simple direct formation of self-assembled N-heterocyclic carbene monolayers on gold and their application in biosensing. *Nat. Commun.* **2016**, *7*, 12654.

12. Wu, C.-Y.; Wolf, W. J.; Levartovsky, Y.; Bechtel, H. A.; Martin, M. C.; Toste, F. D.; Gross, E. High-spatial-resolution mapping of catalytic reactions on single particles. *Nature* **2017**, *541*, 511-515.

13. Levratovsky, Y.; Gross, E. High spatial resolution mapping of chemically-active self-assembled N-heterocyclic carbenes on Pt nanoparticles. *Faraday discussions* **2016**, *188*, 345-353.

14. Dery, S.; Amit, E.; Gross, E. Identifying catalytic reactions on single nanoparticles. *Topics in Catalysis* **2018**, *61*, 923-939.

15. Nguyen, D. T.; Freitag, M.; Körsgen, M.; Lamping, S.; Rühling, A.; Schaefer, A. H.; Siekman, M. H.; Arlinghaus, H. F.; van der Wiel, W. G.; Glorius, F. Versatile Micropatterns of N-Heterocyclic Carbenes on Gold Surfaces: Increased Thermal and Pattern Stability with Enhanced Conductivity. *Angew. Chem.*, *Int. Ed*. **2018**, *57*, 11465-11469.

16. DeJesus, J. F.; Trujillo, M. J.; Camden, J. P.; Jenkins, D. M. N-Heterocyclic Carbenes as a Robust Platform for Surface-Enhanced Raman Spectroscopy. *J. Am. Chem. Soc.* **2018**, *140*, 1247-1250.

17. Dery, S.; Kim, S.; Haddad, D.; Cossaro, A.; Verdini, A.; Floreano, L.; Toste, F. D.; Gross, E. Identifying site-dependent reactivity in oxidation reactions on single Pt particles. *Chem. Sci.* **2018**, *9*, 6523-6531.

18. Wang, G.; Rühling, A.; Amirjalayer, S.; Knor, M.; Ernst, J. B.; Richter, C.; Gao, H.-J.; Timmer, A.; Gao, H.-Y.; Doltsinis, N. L.; Glorius, F.; Fuchs, H. Ballbot-type motion of N-heterocyclic carbenes on gold surfaces. *Nat. Chem.* **2016**, *9*, 152.

19. Busetto, E.; Lausi, A.; Bernstorff, S. The high-energy monochromator for the ALOISA beamline at Elettra. *Rev. Sci. Instrum.* **1995**, *66*, 2078-2081.

20. Floreano, L.; Naletto, G.; Cvetko, D.; Gotter, R.; Malvezzi, M.; Marassi, L.; Morgante, A.; Santaniello, A.; Verdini, A.; Tommasini, F.; Tondello, G. Performance of the grating-crystal monochromator of the ALOISA beamline at the Elettra Synchrotron. *Rev. Sci. Instrum.* **1999**, *70*, 3855-3864.

21. Cossaro, A.; Dell'Angela, M.; Verdini, A.; Puppin, M.; Kladnik, G.; Coreno, M.; de Simone, M.; Kivimäki, A.; Cvetko, D.; Canepa, M.; Floreano, L. Amine Functionalization of

Gold Surfaces: Ultra High Vacuum Deposition of Cysteamine on Au(111). *J. Phys. Chem. C* **2010**, *114*, 15011-15014.

22. Song, X.; Ma, Y.; Wang, C.; Dietrich, P. M.; Unger, W. E. S.; Luo, Y. Effects of Protonation, Hydrogen Bonding, and Photodamaging on X-ray Spectroscopy of the Amine Terminal Group in Aminothiolate Monolayers. *J. Phys. Chem. C* **2012**, *116*, 12649-12654.

23. Wang, J.; Neoh, K. G.; Kang, E. T. Comparative study of chemically synthesized and plasma polymerized pyrrole and thiophene thin films. *Thin Solid Films* **2004**, *446*, 205-217.

24. Jansen, R. J. J.; van Bekkum, H. XPS of nitrogen-containing functional groups on activated carbon. *Carbon* **1995**, *33*, 1021-1027.

25. Graf, N.; Yegen, E.; Gross, T.; Lippitz, A.; Weigel, W.; Krakert, S.; Terfort, A.; Unger, W. E. S. XPS and NEXAFS studies of aliphatic and aromatic amine species on functionalized surfaces. *Surf. Sci.* **2009**, *603*, 2849-2860.

26. La, Y.-H.; Jung, Y. J.; Kang, T.-H.; Ihm, K.; Kim, K.-J.; Kim, B.; Park, J. W. NEXAFS Studies on the Soft X-ray Induced Chemical Transformation of a 4-Nitrobenzaldimine Monolayer. *Langmuir* **2003**, *19*, 9984-9987.

27. Siemeling, U.; Memczak, H.; Bruhn, C.; Vogel, F.; Träger, F.; Baio, J.; Weidner, T. Zwitterionic dithiocarboxylates derived from N-heterocyclic carbenes: coordination to gold surfaces. *Dalton Trans.* **2012**, *41*, 2986-2994.

28. Jiang, L.; Zhang, B.; Médard, G.; Seitsonen, A. P.; Haag, F.; Allegretti, F.; Reichert, J.; Kuster, B.; Barth, J. V.; Papageorgiou, A. C., N-Heterocyclic carbenes on close-packed coinage metal surfaces: bis-carbene metal adatom bonding scheme of monolayer films on Au, Ag and Cu. *Chem. Sci.* **2017**, *8*, 8301-8308.

29. Zeng, Y.; Zhang, T.; Narouz, M. R.; Crudden, C. M.; McBreen, P. H., Generation and conversion of an N-heterocyclic carbene on Pt(111). *Chem. Commun.* **2018,** *54*, 12527-12530

30. Tamada, K.; Hara, M.; Sasabe, H.; Knoll, W., Surface Phase Behavior of n-Alkanethiol Self-Assembled Monolayers Adsorbed on Au(111): An Atomic Force Microscope Study. *Langmuir* **1997**, *13*, 1558-1566.

31. Dannenberger, O.; Buck, M.; Grunze, M., Self-Assembly of n-Alkanethiols: A Kinetic Study by Second Harmonic Generation. *J. Phys. Chem. B* **1999**, *103*, 2202-2213.

32. Anderson, M. R.; Evaniak, M. N.; Zhang, M., Influence of Solvent on the Interfacial Structure of Self-Assembled Alkanethiol Monolayers. *Langmuir* **1996**, *12*, 2327-2331.

33. Dai, J.; Li, Z.; Jin, J.; Cheng, J.; Kong, J.; Bi, S., Study of the solvent effect on the quality of dodecanethiol self-assembled monolayers on polycrystalline gold. *J. Electroanal. Chem* **2008**, *624*, 315-322.